XV LATIN-AMERICAN CONGRESS ON ELECTRICITY GENERATION AND TRANSMISSION - CLAGTEE 2024
Mar del Plata, Argentina, November 27th – 29th, 2024

1

Optimal Reactive Power Dispatch of an Industrial Power System with Renewable Energy

G. J. Friedrich[1], A. A. Augusto[1], T. T. Borges[1] and A. F. Schiochet[2]

[1] Universidade Federal Fluminense, Niterói – RJ, Brazil

[2]Universidade Federal de Juiz de Fora, Juiz de Fora – MG, Brazil

e-mail: gustavojacques@id.uff.br, aaaugusto@id.uff.br, thiagotrezza@id.uff.br, eel.afs@gmail.com

Abstract-- **The demand for low-carbon solutions has led major electricity consumers to seek ways of replacing fossil fuel consumption with renewable energy in their processes. The intermittent nature of power generated by key renewable sources has implications for the generation-load balance of the electrical system, especially in weaker grids. This paper presents a case study for a behind-the-meter integration of a photovoltaic (PV) source into a downstream oil and gas industrial electrical system. The developed analysis uses a quasi-static power flow simulation employing Python's library, Pandapower. An Optimal Reactive Power Dispatch (ORPD) algorithm is proposed to control the plant's power factor (PF) at the Point of Interconnection (POI) with the bulk power system and to minimize its main buses voltage magnitude deviations. An Evolutionary Algorithm, called Particle Swarm Optimization (PSO), is applied to run the ORPD, defining the day-ahead setpoints for the plant's existing synchronous generators (SG) controlled voltages, PV inverter reactive power injections, and transformers tap positions. The results showed that the proposed algorithm effectively maintained the POI power factor within regulatory limits while keeping the system bus voltage magnitude within its specified utilization range throughout the daily renewable energy generation curve.**

Index Terms—**Renewable energy sources, Hybrid power system, Industrial power systems, Reactive power control, Particle swarm optimization**

I. NOMENCLATURE

HV – High-voltage.
MV – Medium-voltage.
OLTC – On-load Tap Commuter
RHS – Right Hand Side
USD – United States Dollars

II. INTRODUCTION

Photovoltaic (PV) solar energy has been one of the fastest-growing energy sources in the last decade, with its globally installed capacity increasing from 40 GW in 2010 to 586 GW in 2019 [1]. This trend has been driven primarily by the necessity of adopting low-carbon solutions in response to the impacts of climate change. Furthermore, the continuous reduction in its Levelized Cost of Electricity (LCOE), decreasing 89% between 2010 and 2022, falling from 449 USD/MWh in 2010 to 49 USD/MWh in 2022 [2], is accelerating its application.

The energy produced by PV generation is intrinsically linked to solar irradiation, whose levels fluctuate daily from zero to some maximum value. This intermittent nature directly impacts the electrical system generation-load balance, and its system integration has become a subject of intense study by grid planners. As the share of renewable sources in the generation portfolio increases, new challenges arise, especially those related to power quality. These challenges include problems associated with harmonics, voltage fluctuations and violations, reverse power flow, and electrical equipment protection discoordination [3].

Impact studies aim to identify the effects resulting from the integration of renewable sources on the performance of the electrical system, enabling the formulation of mitigation solutions [4]. One possible approach for these studies is through the quasi-static power flow. This method consists of a sequential series of power flow simulations with a defined periodicity over a specific period of interest. This approach emerges as an alternative to the dynamic simulation methods, which require more detailed modeling and more significant computational effort.

Major oil and gas companies have been urgently searching for ways to reduce their Scope 1 and 2 carbon emissions to comply with international agreements and local agencies' regulations. Electrifying low efficient thermal machines and obtaining electrical energy from renewable sources are among possible alternative measures to achieve these goals. Behind-the-meter integration of renewable sources refers to its installation on the customer side of the utility meter and is a viable approach to oil and gas companies decarbonize its activities. However, its application can lead to power factor and voltage control issues for the industrial electrical system. It is well known that, especially in predominantly inductive networks, reactive power variations strongly affect bus voltage magnitudes [5], which needs to be maintained within electrical equipment and load supply range. In this sense, control strategies must seek to simultaneously control the plant's power factor and bus voltage magnitudes.

While there is a significant amount of work evaluating the impacts of renewable sources on distribution and transmission electrical systems, the interest of large industrial consumers in utilizing them within their internal electrical systems is still recent, underscoring the need for more research and publications exploring such a topic [6]-[7].

This paper aims to assess the electrical performance of a behind-the-meter PV source integration in a grid-connected industrial refinery electrical system already containing internal

XV LATIN-AMERICAN CONGRESS ON ELECTRICITY GENERATION AND TRANSMISSION - CLAGTEE 2024
Mar del Plata, Argentina, November 27th – 29th, 2024

2

generation based on thermal source. The analysis will focus on the power factor (PF) hourly variations at the point of interconnection (POI) with the external grid and on the system bus voltage fluctuations. An Optimal Reactive Power Dispatch (ORDP) strategy is proposed for controlling the plant's POI power factor and the system's bus voltage magnitude deviations. The proposed control strategy uses an Evolutionary Optimization Algorithm called Particle Swarm Optimization (PSO) to adjust various electrical system's continuous and discrete control variables. This proposed algorithm will set the plant's fossil-driven synchronous generators (SG) automatic voltage regulators (AVR), PV source inverter reactive power injection, and HV-MV transformers tap positions to accomplish its goals

III. MATERIALS AND METHODS

A. Power flow algorithm

The power flow problem solution involves calculating the voltages and angles at all buses and the power flows through each branch of a given electrical network. Numerous algorithms have been developed for performing this task, with nonlinear programming approaches, especially those based on the Newton-Raphson method, being among the most commonly used. In these approaches, each bus in the electrical network is traditionally classified into one out of three categories: *slack bus* ($V_k\theta_k$), *voltage-controlled bus* (P_kV_k), or *load bus* (P_kQ_k). The designation of each category indicates the predetermined electrical variables associated with it. The problem is then formulated on the mismatch equations between the power injections calculated through the solution of bus's voltage magnitude and angle and the scheduled active (P_k^{sch}) and reactive (Q_k^{sch}) powers, which must equal. Active power mismatch equations can be solved for voltage-controlled buses (N_{PV}) and load buses (N_{PQ}), while reactive power mismatch equations can be solved for load buses. Equations (1) and (2) present the power mismatch equations for an arbitrary bus 'm' of an N-bus electrical network, where G_{mn} and B_{mn} are the branch's conductance and susceptance between buses 'm' and 'n', respectively.

$$\Delta P_m = P_m^{sch} - V_m \sum_{n=1}^{N} V_n(G_{mn}\cos\theta_{mn}+B_{mn}\sin\theta_{mn}) = 0 \quad (1)$$

$$\Delta Q_m = Q_m^{sch} - V_m \sum_{n=1}^{N} V_n(G_{mn}\sin\theta_{mn}-B_{mn}\cos\theta_{mn}) = 0 \quad (2)$$

Equations (1) and (2) are iteratively solved by matching it with the product between the angles and voltages magnitudes deviations and the power equations Jacobian matrix (**J**) [8].

$$[\mathbf{J}]\begin{bmatrix}\Delta\boldsymbol{\theta}\\\Delta\mathbf{V}\end{bmatrix}=\begin{bmatrix}\Delta\mathbf{P}\\\Delta\mathbf{Q}\end{bmatrix} \quad (3)$$

Where vectors $\Delta\mathbf{P}$ and $\Delta\mathbf{Q}$ are formulated as per indicated in (1) and (2), and angles and voltage magnitudes mismatches are

calculated as per (4) and (5), where the index i represents the algorithm iteration.

$$\theta_m^{i+1}=\theta_m^i+\Delta\theta_m \quad (4)$$

$$V_m^{i+1}=V_m^i+\Delta V_m \quad (5)$$

B. Optimal Reactive Power Dispatch (ORPD)

The Optimal Reactive Power Dispatch (ORPD) is a multi-objective mixed-integer nonlinear (MINLP) sub-problem of optimal power flow (OPF) that usually consists of minimizing electrical system power losses while enhancing its voltage profile [9]. In order to achieve these goals, the ORPD algorithm adjusts the electrical system's continuous and discrete variables for controlling network reactive power flow. Variables typically optimized by the ORPD algorithm are the generator's voltages, the transformer's taps, and reactive power injection setpoint by compensation devices (e.g., capacitor banks, static var compensators, synchronous condensers).

C. Particle Swarm Optimization (PSO)

J. Kennedy and R. Eberhart invented Particle Swarm Optimization (PSO) algorithm in 1995 [10]. The technique was inspired by the behavior of creatures like fish schooling and bird flocking, where each agent's response is dictated by its own and the group's experiences. This method has already been successfully applied for solving an electrical system ORPD problem [11].

Each possible solution for the objective function minimization (or maximization) is called a particle in this method. The particles are randomly initiated and then move along the n-dimensional search space. Every particle has a position (**X**) and a velocity (**V**), which are updated at each iteration [12]. The updates are based on the particle's best position (*pbest*$_i$) and group's best position (*gbest*), as per indicated in (6) and (7), for an arbitrary 'i' iteration:

$$V_k^{i+1}= \omega_k^i V_k^i+c_1 rand_1\big(pbest_k^i - X_k^i\big) \\ + c_2 rand_2\big(gbest^i - X_k^i\big) \quad (6)$$

$$X_k^{i+1}=X_k^i + C.V_k^{i+1} \quad (7)$$

Where:

- V_k^i, V_k^{i+1} are the particle 'k' velocities at iterations 'i' and 'i+1', respectively.
- X_k^i, X_k^{i+1} are the particle 'k' positions at iterations 'i' and 'i+1', respectively.
- $pbest_k^i$ is the particle 'k' best position at iteration 'i'.
- $gbest^i$ is the group best position at iteration 'i'
- c_1, c_2 are the cognitive and the social coefficients, respectively.
- ω_k^i is the particle 'k' inertia coefficient at iteration 'i'.
- C is the constriction factor.
- $rand_1$, $rand_2$ are random numbers in range [0,1].

The inertia coefficient (ω_k^i) balance the algorithm's local and global search. Experience indicates that best results are obtained if its value is updated between a maximum (ω_{max}) and minimum (ω_{min}) as a linear function of iteration value 'i', as shown in (8) [13].

$$\omega_k^i = \omega_{max} - \frac{\omega_{max} - \omega_{min}}{Number_{iteration}} \times \text{Iteration} \qquad (8)$$

The constriction factor (C) is another parameter used for algorithm result stability and is calculated according to (9) [14].

$$C = \frac{2}{\left|2 - \varphi - \sqrt{\varphi^2 - 4\varphi}\right|}, \text{ where } \varphi = c_1 + c_2, \varphi > 4 \qquad (9)$$

D. Industrial Electrical System Generation Dispatch

Typical downstream oil and gas industrial plants have Combined Heat and Power (CHP) schemes that use fossil fuel and process waste gases to generate steam, heat, and electricity simultaneously. These plants are usually connected to the bulk power system, enabling the sale or purchase of electricity whenever required. Overall, the internal electrical generation active power dispatch for these plants involves a complex optimization problem, where multiple variables need to be accounted (e.g., fuel and electricity wholesale prices, plant's steam, heat, and electricity demands, CO_2 emissions, viable operation mode) [15].

While SG active power dispatch is limited by prime mover capability, reactive power dispatch is limited by three main variables: (a) armature current; (b) field current; and (c) end region limit [16]. These three limits, along with the generator's prime mover limit, compose into the capability curve, which indicates generators permissible area for active and reactive power dispatch. Fig. 1 graph shows a cylindrical rotor synchronous generator typical reactive power capability curve [17]. As can be depicted, the generator power factor, and its reactive power dispatch limit, depends on the active power generation.
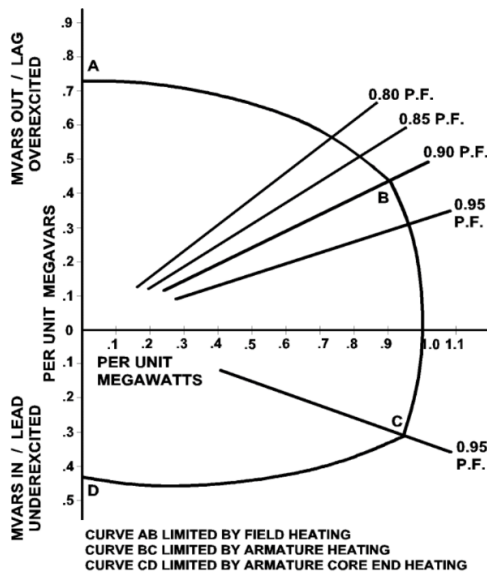

Fig. 1 Typical reactive power capability curve for a synchronous generator.

Electrical system's reactive power dispatch usually aims to minimize losses while enhancing bus voltage profile. While bulk power system transmission lines span large distances, industrial electrical feeders tend to be shorter, making these last electrical system power losses significantly lower. For these last system's, the reactive power dispatch is oriented to maintain the system's bus voltage at an adequate utilization level while maintaining its POI with external grid within regulatory limits. Brazil's electrical system national operator (ONS) sets a minimum 0.95 power factor threshold for consumers directly connected to the transmission system, which is the case for the majority of large national oil and gas industrial unities.

The voltage range for industrial equipment typically lies within the 0.95 to 1.05 pu range. Given that an industrial electrical system typically has a radial topology, its end load bus tends to have lower voltage when compared to primary distribution buses. For this reason, primary distribution bus voltages are expected to operate just above the 1.00 pu level, to compensate for network voltage drops

E. Photovoltaic inverter reactive power injection

Many standards and codes regarding grid-connected PV inverters establish requirements for power factor and reactive power injection at the grid connection point. The Brazilian Standard for distribution-connected PV inverters (ABNT NBR 16149) requires that inverters with rated power above 6kW must be able to operate with a power factor from 0.90 lagging to 0.90 leading when output active power is within 20% to 90% of its rated value [18]. Fig. 2 graph shaded gray area shows Standard ABNT NBR 16149 photovoltaic inverter operating locus [19].
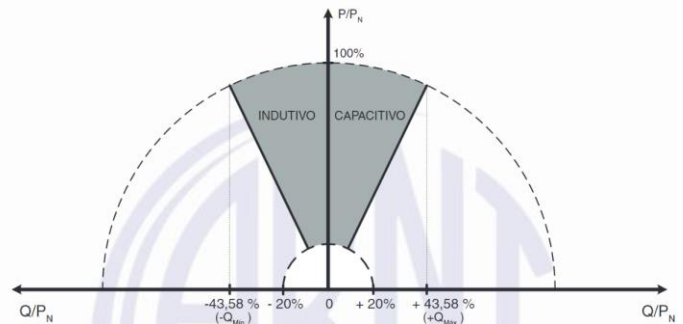

Fig. 2 Standard ABNT NBR 16149 photovoltaic inverter operating area.

IV. CASE STUDY

A. Study case application for the ORPD

A study case will be conducted in a refinery industrial electrical system exploring a behind-the-meter installation of a photovoltaic source. This study case will focus on applying a ORPD routine for defining system's different sources reactive power dispatch. The following sections will present the electrical system modelling and optimization algorithm applied methodology.

B. Network Modelling

Fig. 3 shows the studied industrial electrical system one-line

XV LATIN-AMERICAN CONGRESS ON ELECTRICITY GENERATION AND TRANSMISSION - CLAGTEE 2024
Mar del Plata, Argentina, November 27th – 29th, 2024

4

diagram. It consists in a grid-connected HV sector (138kV) and three MV primary distribution (13.8kV) islands. Each island is connected to the HV sector by one 40MVA 138-13.8kV power transformer (T1, T2, and T3) equipped with OLTC. Island's 1 and 2 are also supplied by steam moved synchronous generators (G1, G2, G3, G4, and G5). The network model also contains a few air-core reactors for short-circuit current limitation and electrical cable for panels interconnection. Table I shows data for Fig. 3 system's power transformers and air-core reactors and Table II shows data for the electrical cables.

TABLE I
TRANSFORMER AND AIR-CORE REACTOR DATA

Id.	Rated Power	Reactance	X/R
T_1, T_2 and T_3	40 MVA	12.5%	30
X_{2-3}, X_{2-4} and X_{2-5}	20 MVA	0.42Ω/phase	50
X_{7-8}	20 MVA	0.45Ω/phase	50
X_{8-9} and X_{8-10}	20 MVA	0.40Ω/phase	50

TABLE II
ELECTRICAL CABLE DATA

Id.	Resistance	Reactance	Length
L_3, L_4 and L_5	0.0850 Ω/km	0.1120 Ω/km	0.2 km
L_8 and L_9	0.0850 Ω/km	0.1120 Ω/km	0.2 km
L_{11}	0.0850 Ω/km	0.1120 Ω/km	0.5 km
L_2, L_6 and L_{10}	0.0760 Ω/km	0.0646 Ω/km	2.0 km

Python's open-source library 'Pandapower' [20] is used for electrical system modelling, control and simulation. This platform is chosen due to its integration with other Python's third parties' libraries such as 'Pandas' and 'NumPy', allowing easy implementation of external files reading and optimization algorithms routines.
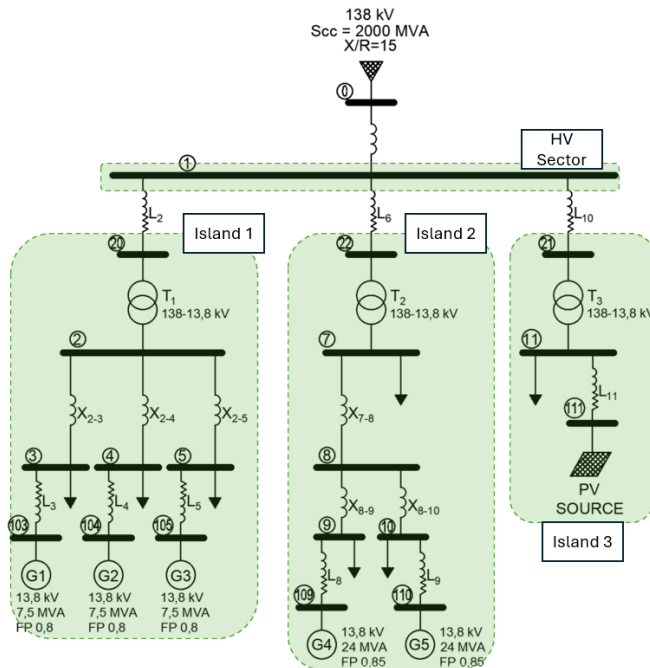

Fig. 3 Industrial system electrical one-line diagram.

C. Synchronous Generators modelling

The methodology adopted in this paper for the synchronous generators (SG) modelling considers their active power dispatch as fixed, regardless of the renewable energy penetration, with values according to Table III. This premise enforces that the interchange with the bulk power system is responsible for absorbing the active power fluctuations caused by the PV source penetration. This assumption significantly reduces the analysis complexity since it dismisses the necessity of running a CHP optimization in parallel with the ORPD at each simulation time step. This simplification is justified by the fact that the main focus of this paper is to assess the reactive power dispatch problem. If necessary, it would be easy to adapt the proposed control algorithm to account for simultaneous changes in synchronous generators' active power dispatch.

TABLE III
INTERNAL GENERATION ACTIVE POWER DISPATCH

Id.	Active Power dispatch [MW]	Reactive Power Limit [Mvar]
G_1, G_2 and G_3	6.0	6.375
G_4 and G_5	11	12.35

The proposed ORPD algorithm will use SG's terminal voltage as a control variable to maintain PF at the POI with the bulk power system within the strict regulatory limits, as discussed in next sections. The SGs setpoint references shall be updated at each time step of simulation by the optimization algorithm. In an actual system operation, these variables would be controlled by regulating SG's AVR setpoint, which typically has a fast response.

SG reactive power dispatch limit shall be taken as constraints when formulating the power flow algorithm, according to the values shown in Table III. Since its active power dispatch is maintained constant throughout simulation, so is its conjugated reactive power limit.

D. Transformers OLTC modelling

Industrial main HV-MV transformers are typically equipped with OLTC, which enables changing taps while the transformer is energized. As its primary winding is connected to a bus whose voltage is dictated by the external grid and is only slightly affected by the industrial internal system, transformer tap commutation can control its branch's reactive power flow and secondary voltage.

The developed model considers transformer taps as discrete control variables, meaning that the optimization must simultaneously handle continuous and discrete variables. Transformers T1, T2 and T3 limits are between ±10% range with 1.25% step ratio.

E. Load modelling

The electrical loads consist of the plant's area substations that feed industrial equipment (e.g. pumps, compressors, heaters). For model simplicity, they were grouped in the primary distribution system main buses as constant power loads (ZIP model). Table IV shows the electrical loads power demands at each main primary distribution bus and plant's total

XV LATIN-AMERICAN CONGRESS ON ELECTRICITY GENERATION AND TRANSMISSION - CLAGTEE 2024
Mar del Plata, Argentina, November 27th – 29th, 2024

5

power demand.

Bus	Active Power [MW]	Reactive Power [Mvar]
3	5.4	1.8
4	11.7	5.4
5	8.1	4.5
7	20	14
9	10	4.0
10	7.5	3.0
11	16.5	10.5
Total	79.2	43.2

To account for the plant's daily normal load variations, Table IV power demands will be varied between -5% and +5% following a gaussian distribution between adjacent time steps.

F. Photovoltaic source modelling

The PV source is modeled as active and reactive power injections at Bus 111 of Fig. 3 electrical system. This bus is considered a load-type bus in the formulation of the power flow problem, and the active and reactive power injections are updated at each simulation time step. Assumed PV source active power injections are indicated in generation profile curves plotted in Fig. 4 graph.

The utilized data was collected from an existing PV plant located in the state of Minas Gerais, Brazil, for the average generation in January 2022. This data is publicly available on the Brazilian National Operator (ONS) website. The plant's original generation values were scaled to match the proposed PV source rated powers at its daily peak under three different scenarios:

- Scenario 1: 10 MW.
- Scenario 2: 20 MW.
- Scenario 3: 30 MW.

Simulation is performed with hourly time steps between 05:00 and 19:00, as shown in Fig. 4, resulting in 15 ORPD runs for each scenario.
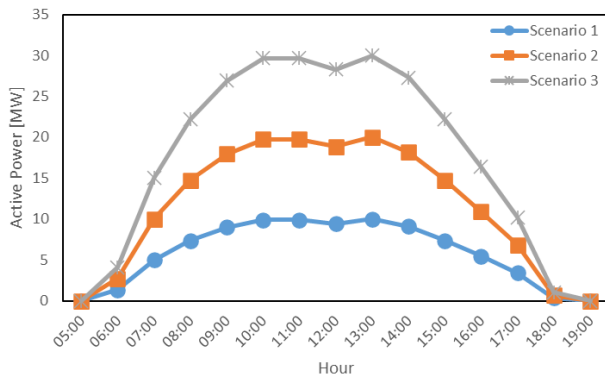

Fig. 4 Photovoltaic daily generation profile.

The PV inverters are considered to be oversized so that the

plant is capable of providing reactive power even during its daily peak generation. This means that PV panels peak generation (10 MW, 20 MW or 30 MW) corresponds to 90% of inverter's permissible power output indicated in Fig. 2 graph.

G. Developed Model Validation

To guarantee coherent results, the Pandapower developed model was compared with a specific model developed in the electrical simulation software Power Tools for Windows (PTW). Load and generation were set to equivalency between the two models, and voltage values, in kilovolts, for main buses are shown in Table V.

Bus	Pandapower	PTW	Var. (%)
1	137810.2298	137810.2	0.0001%
2	13933.08956	13933.07	0.0001%
3	14060.50688	14060.51	0.0000%
4	14033.30228	14033.33	-0.0002%
5	14050.07211	14050.06	0.0001%
7	13804.43492	13804.79	-0.0026%
8	13976.14623	13976.25	-0.0007%
9	14052.12553	14052.13	0.0000%
10	14053.74427	14053.75	0.0000%
11	14259.7546	14259.79	-0.0002%
20	137824.7725	137824.7	0.0001%
21	137818.3284	137818.3	0.0001%
22	137809.5685	137809.5	0.0001%
111	14340.45749	14340.5	-0.0003%

H. Optimal Reactive Power Dispatch (ORPD) Formulation

Two objectives were chosen for formulating the optimization function: (a) maintaining the plant's power factor at the POI with the bulk power system at 1.00, and (b) minimizing the voltage deviations at a few selected buses (2, 7 and 11). Equation (11) presents the objective function $f(x, y)$ chosen to be minimized by the ORPD algorithm, where (x, y) are the system's continuous and discrete state variables. Variable PF_{POI} represents the plant's power factor at the point of interconnection with the bulk power system and V_n is the selected bus voltage magnitude, in per unit.

$$f(x, y) = k_1|1.00 - PF_{POI}| + k_2 \sum_{n=2,7,11} |1.02 - V_n| \quad (11)$$

Being a metaheuristic optimization procedure, PSO does not guarantee exact solution convergence, unlike mathematical programming optimization methods (e.g., linear and nonlinear programming). For this reason, it was chosen to define the objective function so as to maintain the PF_{POI} close to unity, ensuring that program convergence natural mismatches still remain above the acceptable 0.95 regulatory threshold.

The voltage deviation index (second objective) is only calculated for buses 2, 7, and 11, which are located at the secondaries of the electrical system's main HV-MV transformers. This condition was chosen to avoid OLTC control

XV LATIN-AMERICAN CONGRESS ON ELECTRICITY GENERATION AND TRANSMISSION - CLAGTEE 2024
Mar del Plata, Argentina, November 27th – 29th, 2024

6

instability. Also, the objective function voltage reference for deviation calculation is chosen to be 1.02 pu to ensure that the primary distribution buses voltage magnitudes are above 1.00 pu level.

Coefficients k_1 and k_2 balance the two RHS sub-equations mismatches. They are important to ensure that all objectives are equally achieved by optimization.

Equation (11) objective function will be minimized by applying the PSO algorithm described in the previous section. The following variables were chosen for controlling the electrical system's reactive power to achieve this goal:

- X_1: Generators G1, G2 and G3 controlled voltage.
- X_2: Generators G4 and G5 controlled voltage.
- X_3: Transformer T1 tap position.
- X_4: Transformer T2 tap position.
- X_5: Transformer T3 tap position.
- X_6: PV source reactive power injection.

Electrical Islands 1 (G1, G2, and G3) and 2 (G4 and G5) SG had their controlled voltages coupled into the same PSO particles to avoid potential instability caused by intra-island control disputes. This means the PSO algorithm perceives their voltage magnitudes as one single variable and seeks optimization by manipulating them simultaneously.

Since the control variables can be configured in multiple ways to satisfy the objective function shown in (11), it is important to avoid extreme oscillation in their setpoints between adjacent time steps. This can be achieved by initiating PSO particles within a close range of the previous time step global best positions. Traditional application of PSO initiates each particle position of the **X** vector randomly within the control variables range. However, to avoid significant variations between adjacent time steps and to guarantee better variable continuity, particles associated with SGs voltages and transformers tap setpoints are to be initiated following a gaussian distribution between 0.90 and 1.10 times the previous time step's best parameter. This rule's only exception is in the daily first iteration (05:00), where particles are initiated according to the traditional algorithm application.

A second measure adopted to improve control variable stability between adjacent time steps is to only adjust the HV-MV transformers T1, T2 and T3 tap position when the voltage magnitudes of buses 2,7 and 11, respectively, falls out of the specified 1.00 to 1.03 pu range deadband between adjacent time steps.

I. Simulation flowchart

Fig. 5 flowchart illustrates the developed simulation procedure. Firstly, the PV active power generation data is read from an external Excel spreadsheet and stored in a Python data frame type variable. Then, the electric network is initiated, modeling Fig. 3 electrical system. The ORPD for each time step is run within a loop that systematically updates the system's loads and the PV active power generation. The PSO algorithm is first run for each time step without adjusting the transformer's

taps. If the optimization resultant value for buses 2, 7 or 11 voltage magnitude falls out of the 1.00 to 1.03 pu range, then a second optimization is performed, and the transformers taps are also adjusted along with SG voltages and PV source reactive power injection. The optimized results for each time steps are saved and later exported to an Excel spreadsheet.
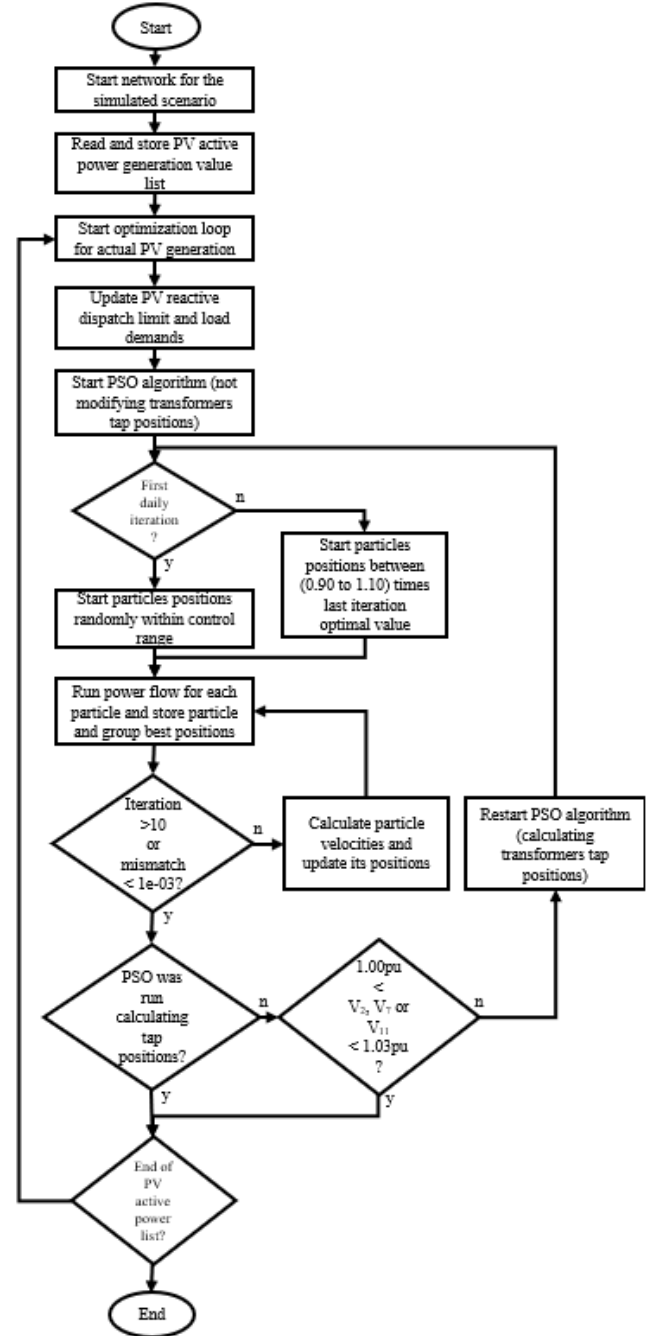

Fig. 5 Simulation flowchart.

V. RESULTS AND DISCUSSIONS

A. Optimization algorithm test parameters and tolerance

The PSO algorithm was set to run with 30 particles, 10 iterations, and with a 2.05 value for the cognitive (c_1) social (c_2) coefficients. The inertia coefficient was set to vary linearly

XV LATIN-AMERICAN CONGRESS ON ELECTRICITY GENERATION AND TRANSMISSION - CLAGTEE 2024
Mar del Plata, Argentina, November 27th – 29th, 2024

7

between 0.9 and 0.4 from the first to the last iteration, following (5). Objective function f(x,y) balancing constants k_1 and k_2 were set to 1.00 and 3.00, respectively. These parameters were all obtained through pre-testing.

The following constraints were imposed for system's control variables:

- 1.00 pu ≤ V_{G1}, …, V_{G5} ≤ 1.05 pu
- 0 ≤ Q_{G1}, …, Q_{G3} ≤ 6.375 Mvar
- 0 ≤ Q_{G4}, Q_{G5} ≤ 12.35 Mvar
- -10% ≤ $OLTC_{T1}$, … , $OLTC_{T3}$ ≤ +10%
- 0 ≤ Q_{PV} ≤ 0.435 x P_{PV}, if P_{PV} ≥ 0.2 x $P_{PV,MAX}$
- Q_{PV} = 0, if P_{PV} < 0.2 x $P_{PV,MAX}$

Where V_{G1}, …, V_{G5} are the SG voltages, Q_{G1}, …, Q_{G5} are the SG reactive power dispatch, $OLTC_{T1}$, … , $OLTC_{T3}$ are the HV-MV transformers tap positions, and Q_{PV} and P_{PV} are the PV source reactive and active power. The SG voltages and PV source reactive power injection are permitted to vary continuously between constraints while the HV-MV transformers tap positions are only permitted to vary in steps of ±1.25%.

Power flow simulations were performed with 1e-08 tolerance using the Newton-Raphson solution method. PSO algorithm was performed until objective mismatch was inferior to 1e-03 or iteration achieved ten attempts.

B. Processing system characteristics

Simulation was run on a machine equipped with a x64 system with 11th Gen Intel(R) Core(TM) i5-1145G7 @ 2.60GHz CPU having 16 GB RAM. Processing time was inferior to 300 seconds in all simulated scenarios.

C. Simulation Results

This section presents numerical results that illustrate the proposed methodology application depicted in Fig. 5 flowchart in Fig. 3 electrical system for all three studied integration scenarios.

Fig. 6 chart shows PF daily variation at the plant's POI with the bulk power system. It can be noticed that in all three scenarios, the ORPD algorithm was efficient in maintaining the plant's PF within regulatory limits. As already expected, the optimization could not keep the PF value closely attached to the 1.00 objective throughout the day. However, the tolerance and number of iterations imposed to the optimization guaranteed that its error stayed below 0.05, ensuring that its value was always kept above the 0.95 threshold.

In order to maintain the PF close to unity, the optimizer had to adjust the system's electrical sources variables to control its reactive power dispatch. The PV source reactive power daily generation profile is graphically shown in Fig. 5 for all three scenarios. It is clear that Scenario 3 PV's reactive power injection was the highest of all scenarios, while Scenario 1 was the lowest. This result is explained due the fact that SG active dispatch setpoints were kept constant, and the plant's interchange with the bulk power system was responsible for the active power fluctuation caused by the PV source penetration.

In Scenario 3, the active power interchange variation with the bulk power system was the highest, meaning a higher reactive power injection would also be required to reduce interchange reactive power and maintain PF at the POI within the constrained boundaries.

Daily voltage magnitude fluctuations in Fig. 3 electrical system are shown in Fig. 8, Fig. 9, and Fig. 10 graphs for Scenarios 1, Scenario 2, and Scenario 3, respectively. Voltage magnitude was monitored for the following few selected buses:

- Island's 1 SG's terminal buses (BUS_3, BUS_4, and BUS_5).
- Island's 2 SG's terminal buses (BUS_9 and BUS_10).
- Island's 1 (BUS_2) HV-MV transformer secondary.
- Island's 2 (BUS_7) HV-MV transformer secondary.
- Island's 3 (BUS_11) HV-MV transformer secondary
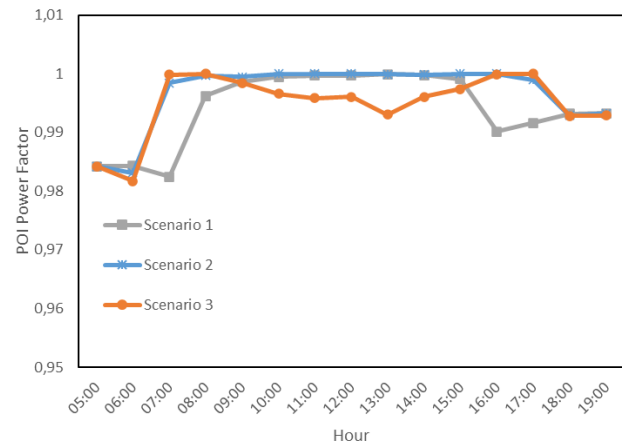- Plant's electrical system main HV (138kV) bus (BUS_1)

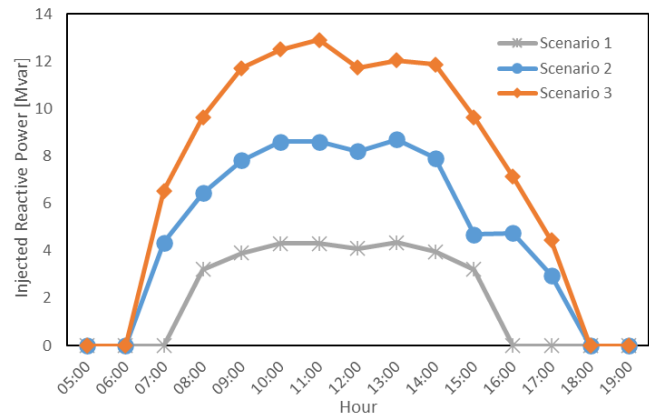Fig. 6 POI power factor daily variation curve.

Fig. 7 PV source reactive power injection daily variations.

Results demonstrated that the ORPD algorithm also achieved its second objective, which was minimizing the system's voltage deviations, seeking to maintain its values within a suitable 0.95 to 1.05 pu operating range. It can be noticed that the system's main buses voltage magnitudes were successfully kept just above the 1.00 pu level, while not exceeding the 1.05 pu threshold at any time. It is worth noticing

that buses 9 and 10 voltage magnitudes are superimposed in Fig. 8, Fig. 9, and Fig. 10 graphs.

Fig. 11 shows the PV generator output PF daily variations. Values are not shown for 05:00 and 19:00 since both active and reactive power are zero for this hour. Results show that the PV source output PF was kept near the 0.90 constraint almost all day, except for the day's first hours, when the generated active power was below the minimum 20% value. In these moments, its output PF is 1.00, meaning no reactive power is generated.

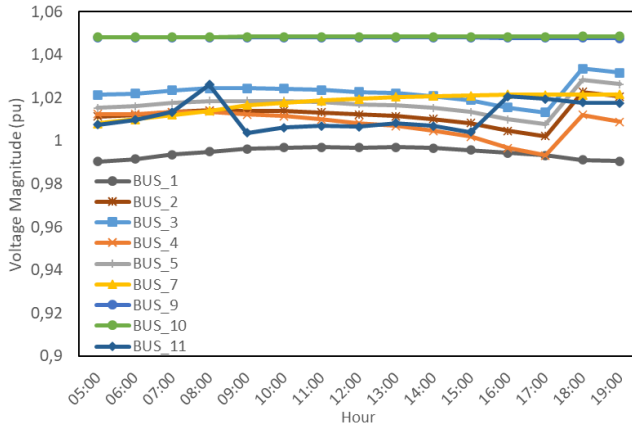Fig. 11 PV generator output power factor.

Fig. 8 Selected buses voltage magnitude daily variations for 10 MW injection.
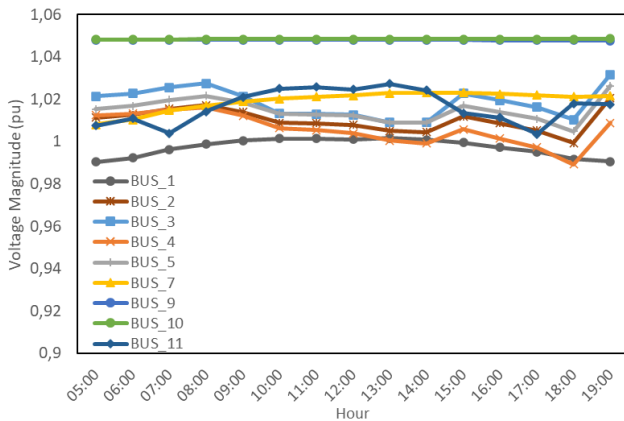

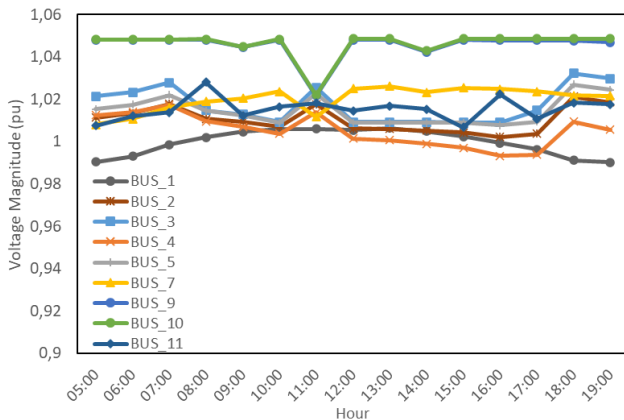Fig. 9 Selected buses voltage magnitude daily variations for 20 MW injection.

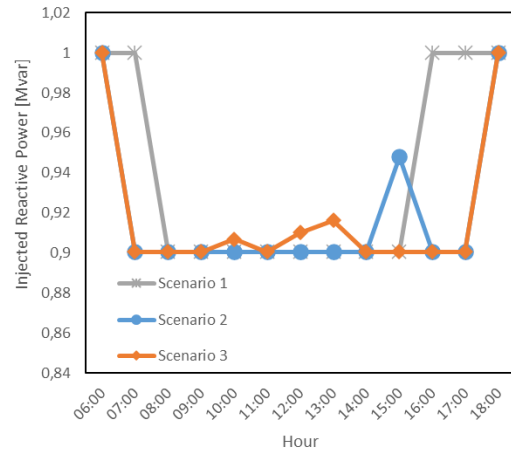Fig. 10 Selected buses voltage magnitude daily variations for 30 MW injection.

While Island 1 SGs had their terminal voltages closely attached around the 1.02 pu setpoint defined in the objective function, Island 2 SG had their voltages raised next to 1.05 pu limit in all three scenarios throughout most of the day. Having a higher voltage at its terminals enabled it to dispatch more reactive power, helping to balance the plant's reactive power flow. Unlike Island 1 SGs, Island 2 SGs were able to maintain their voltages close to its boundary (1.05 pu) and not be penalized by deviating from 1.02 pu objective since bus 7 voltage is not strongly coupled to them because of the voltage drop in the current limiting reactor (X_{7-8}), electrically distancing bus 7 from buses 9 and 10.

A second reason Island's 1 SGs could not increase its voltage was due to reaching its reactive power dispatch limit. As seen in the Fig. 12 graph for Scenario 2, generators G2 and G3 reached the 6.375 MVA reactive power dispatch constraint most of the day. On the other hand, G1 reactive dispatch has not reached the constraint between 08:00 and 15:00, and the reason was due to the fact that Bus 3 power demand, where G1 is connected, is significantly lower than Buses 4 and 5, where G2 and G3 are, respectively, connected. Generators G4 and G5 have not reached the 12.35 MVA reactive power dispatch constraint meaning that they were able to keep its terminal voltage magnitude in the 1.05 pu constraint. Generators G4 and G5 dispatched reactive power at 19:00 was significantly differed from 05:00. This condition is explained by the load demand variations included in the simulation model.
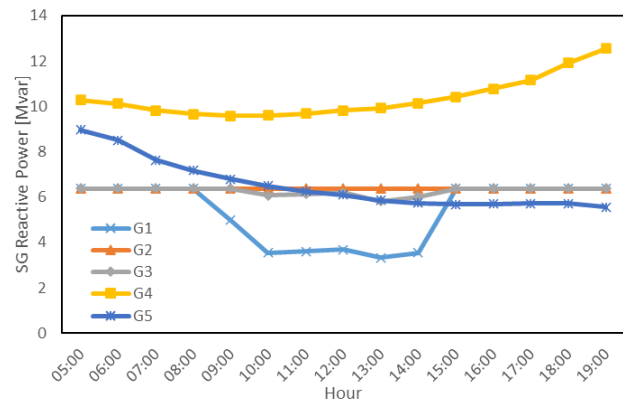

Fig. 12 SG reactive power generation for Scenario 2.

XV LATIN-AMERICAN CONGRESS ON ELECTRICITY GENERATION AND TRANSMISSION - CLAGTEE 2024
Mar del Plata, Argentina, November 27th – 29th, 2024

9

As initially predicted, system's reactive power fluctuations impacted its buses voltages magnitudes making their values raise. Buses overvoltage had to be controlled through transformers OLTC actuation. Table VI shows transformers T1, T2 and T3 tap positions for each simulated time step. These results illustrate necessary transformers tap commutations for maintaining system's voltages within acceptable range, as depicted in the above graphs.

It can be noticed that transformer T3 OLTC had to perform a higher number of daily commutations than the other two, having four daily tap changes for Scenarios 3 and two daily tap change for Scenario 1 and Scenario 2. A higher number of commutations for Scenario 3 can be explained due to the fact that busbar 11 had higher reactive power variation throughout the day, as already indicated in Fig. 7. It should be noted, though, that these quantities of daily commutations are well within the equipment capacity and does not impose maintenance or operation threats.

TABLE VI
TRANSFORMERS TAP POSITIONS (%)

Hour	Scenario 1			Scenario 2			Scenario 3		
	T1	T2	T3	T1	T2	T3	T1	T2	T3
05:00	0.00	-2.50	-5.00	0.00	-2.50	-5.00	0.00	-2.50	-5.00
06:00	0.00	-2.50	-5.00	0.00	-2.50	-2.50	0.00	-2.50	-5.00
07:00	0.00	-2.50	-5.00	0.00	-2.50	-2.50	0.00	-2.50	-2.50
08:00	0.00	-2.50	-5.00	0.00	-2.50	-2.50	0.00	-2.50	-2.50
09:00	0.00	-2.50	-2.50	0.00	-2.50	-2.50	0.00	-2.50	0.00
10:00	0.00	-2.50	-2.50	0.00	-2.50	-2.50	0.00	-2.50	0.00
11:00	0.00	-2.50	-2.50	0.00	-2.50	-2.50	0.00	-2.50	0.00
12:00	0.00	-2.50	-2.50	0.00	-2.50	-2.50	0.00	-2.50	0.00
13:00	0.00	-2.50	-2.50	0.00	-2.50	-2.50	0.00	-2.50	0.00
14:00	0.00	-2.50	-2.50	0.00	-2.50	-2.50	0.00	-2.50	0.00
15:00	0.00	-2.50	-2.50	0.00	-2.50	-2.50	0.00	-2.50	0.00
16:00	0.00	-2.50	-5.00	0.00	-2.50	-2.50	0.00	-2.50	-2.50
17:00	0.00	-2.50	-5.00	0.00	-2.50	-5.00	0.00	-2.50	-2.50
18:00	-2.50	-2.50	-5.00	-2.50	-2.50	-5.00	-2.50	-2.50	-5.00
19:00	-2.50	-2.50	-5.00	0.00	-2.50	-5.00	-2.50	-2.50	-5.00

An additional simulation for the three scenarios was conducted exploring the SG capacity of maintaining POI power factor without PV source reactive power injection aid (e.g. Q_{PV} =0). Fig. 13 graph shows POI power factor results for this simulation.

The plant's SGs were only capable of maintaining system's POI power factor above 0.95 in Scenario 1, where renewable energy penetration was the lowest, demonstrating the importance of PV inverter having reactive power injection capacity. Voltage magnitude and reactive power dispatch constraints prevented the plant's SGs to solely adjust its control variables in order to achieve objective function goal.
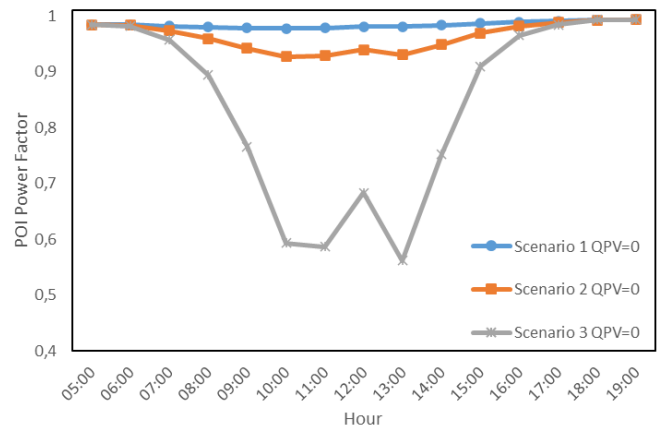

Fig. 13 POI power factor with PV source only injecting active power.

VI. CONCLUSIONS AND FUTURE WORK

Industrial systems operators shall face new challenges with potential behind-the-meter integration of renewable energy within their electrical systems. Existent operational philosophies and control strategies must be updated to accommodate these electrical generation technologies, which possess distinct characteristics from today's applied thermal sources. The development of impact studies as part of basic engineering design is paramount for guaranteeing the system's safe and efficient integration of the renewable sources in the industrial electrical systems.

The present paper developed a case study on a behind-the-meter integration of a PV source into an industrial electrical system. The main focus was to define a strategy for optimizing the reactive dispatch of all electrical system sources, including not only the PV source to be integrated but also the existing thermal SG. The analysis sought to identify and correct the most significant impacts on the system's static operation, mainly identifying the following two effects:

- Reduction in plant's POI with bulk power system power factor as the PV source injects active power throughout the day.
- Bus overvoltage as the industrial electrical system primary MV distribution is a predominantly inductive network and sensitive to reactive power disbalances.

The reduction in plant's power factor was mitigated by controlling the injection of reactive power from its multiple sources, thereby simultaneously decreasing the demands for both active and reactive power at the point of connection with the external grid. The PV source connection bus overvoltage was solved by adjusting the plant's transformers' taps through its OLTC.

The proposed algorithm was shown efficient in achieving its goals, that was maintaining plant's POI power factor within regulatory limits, while keeping bus voltage magnitudes at acceptable levels. It is expected that it can serve as a tool for industrial electrical system operator plan its daily operation.

For future work, it is suggested that a contingency analysis

be run, analyzing its implications for the system's ability to maintain voltage magnitude at its buses. In these cases, other indexes could be applied to the objective function, such as L-index for voltage stability. A second route for future improvement would be comparing the PSO results with other optimization algorithm for solving the ORPD.

VII. REFERENCES

[1] C. Wu, X. P. Zhang, and M. Sterling, "Solar power generation intermittency and aggregation", *Sci Rep* **12**, 1363 (2022). https://doi.org/10.1038/s41598-022-05247-2.

[2] IRENA, *Renewable Power Generation Costs in 2022*, International Renewable Agency, Abu Dhabi, 2023. Available: https://www.irena.org/-/media/Files/IRENA/Agency/Publication/2023/Aug/IRENA_Renewable_power_generation_costs_in_2022.pdf?rev=cccb713bf8294cc5bec3f870e1fa15c2.

[3] O. Gandhi, D. S. Kumar, C. D. Rodríguez-Gallegos, and D. Srinivasan, "Review of power system impacts at high PV penetration Part I: Factors limiting PV penetration", *Solar Energy*, vol. 210, pp. 181-201, Nov. 2020. https://doi.org/10.1016/j.solener.2020.06.097.

[4] R. J. Broderick, J. E. Quiroz, M. J. Reno, A. Ellis, J. Smith, and R. Dugan, "Time Series Power Flow Analysis for Distribution Connected PV Generation", Sandia National Laboratory, Albuquerque, NM, Sandia Report SAND2013-0537, Jan. 2013. Available: https://energy.sandia.gov/wp-content/gallery/uploads/SAND_Time-Series-Power-Flow-Analysis-for-Distribution-Connected-PV-Generation.pdf.

[5] O. I. Elgerd, *Electric Energy System Theory*, McGraw Hill, 1971, pp. 60-62.

[6] A. A. A. Meola, Z. McKinney, R. Rangel, and P. Collie, "Integrating renewable energy behind the meter in upstream oil and gas operations – Part I" in *2022 IEEE IAS Petroleum and Chemical Industry Technical Conference (PCIC)*, Denver, CO, USA, pp. 7-16. doi: 10.1109/PCIC42668.2022.10181295.

[7] S. Fasoli, P. Cormio, R. Lauricella, and M. Marchesini, "First Oil & Gas Application of a Hybrid Power Plant Integrating: Solar PV - Energy Storage – Conventional Power Generation (GTG)," in *2021 Petroleum and Chemical Industry Conference Europe (PCIC Europe)*, Copenhagen, Denmark, 2021, pp. 1-7, doi: 10.23919/PCICEurope50407.2021.9805425.

[8] J. J. Grainger, W. D. Stevenson, Jr, *Power System Analysis*, McGraw Hill, 1994, pp. 329-355.

[9] S.A. Adegoke, Y. Sun, Z. Wang, O. Stephen, "A mini review on optimal reactive power dispatch incorporating renewable energy sources and flexible alternating current transmission system", *Electr Eng* (2024). https://doi.org/10.1007/s00202-023-02199-2.

[10] J. Kennedy, and R. Eberhart, "Particle swarm optimization," *Proceedings of ICNN'95 - International Conference on Neural Networks*, Perth, WA, Australia, 1995, pp. 1942-1948 vol.4, doi: 10.1109/ICNN.1995.488968.

[11] S. Chenniappan, S. Padmanaban, S. Palanisamy, *Power Systems Operation with 100% Renewable Energy Sources*, Elsevier, 2023, pp. 72-73.

[12] K. Ben Oualid Medani and S. Sayah, "Optimal reactive power dispatch using particle swarm optimization with time varying acceleration coefficients," *2016 8th International Conference on Modelling, Identification and Control (ICMIC)*, Algiers, Algeria, 2016, pp. 780-785, doi: 10.1109/ICMIC.2016.7804219.

[13] Y. Shi and R. Eberhart, "A modified particle swarm optimizer," *1998 IEEE International Conference on Evolutionary Computation Proceedings. IEEE World Congress on Computational Intelligence (Cat. No.98TH8360)*, Anchorage, AK, USA, 1998, pp. 69-73, doi: 10.1109/ICEC.1998.699146.

[14] R. C. Eberhart and Y. Shi, "Comparing inertia weights and constriction factors in particle swarm optimization," Proceedings of the 2000 Congress on Evolutionary Computation. CEC00 (Cat. No.00TH8512), La Jolla, CA, USA, 2000, pp. 84-88 vol.1, doi: 10.1109/CEC.2000.870279.

[15] S. Mitra, L. Sun, I. E. Grossmann, "Optimal scheduling of industrial combined heat and power plants under time-sensitive electricity prices," *Energy*, vol. 54, pp. 194-211, Jun. 2013. https://doi.org/10.1016/j.energy.2013.02.030.

[16] P. S. Kundur, O. P. Malik, *Power System Stability and Control*, Second Edition, New York: McGraw Hill Education, 2022, pp. 153-157.

[17] "IEEE Standard for Cylindrical-Rotor 50 Hz and 60 Hz Synchronous Generators Rated 10 MVA and Above," in *IEEE Std C50.13-2014 (Revision of IEEE Std C50.13-2005)* , vol., no., pp.1-63, 9 May 2014, doi: 10.1109/IEEESTD.2014.6811137.

[18] H. H. Figueira, H. L. Hey, L. Schuch, C. Rech and L. Michels, "Brazilian grid-connected photovoltaic inverters standards: A comparison with IEC and IEEE," *2015 IEEE 24th International Symposium on Industrial Electronics (ISIE)*, Buzios, Brazil, 2015, pp. 1104-1109, doi: 10.1109/ISIE.2015.7281626.

[19] *Photovoltaic (PV) systems – Characteristics of the utility interface*, ABNT NBR 16149, Associação Brasileiras de Normas Técnicas, Rio de Janeiro, RJ, Brasil, Mar, 2013.

[20] L. Thurner, A. Scheidler, F. Schäfer, J. H. Menke, J. Dollichon, F. Meier, S. Meinecke, M. Braun, "Pandapower—An Open-Source Python Tool for Convenient Modeling, Analysis, and Optimization of Electric Power Systems," in IEEE Transactions on Power Systems, vol. 33, no. 6, pp. 6510-6521, Nov. 2018, doi: 10.1109/TPWRS.2018.2829021.

VIII. BIOGRAPHIES

Gustavo Jacques Friedrich holds a bachelor's degree (2019) in electrical engineering at the Federal University of Rio Grande do Sul (UFRGS), Brazil. He is currently pursuing his master's degree in electrical engineering at the Fluminense Federal University (UFF), Brazil. Since 2022 he has been working at PETROBRAS as an equipment engineer. He is interested in the following research areas: renewable energy, power system dynamics and optimization of electrical systems.

Andre Abel Augusto (S'13-M'15) received the D. Sc. degree from the Institute of Computing, Fluminense Federal University (UFF), Rio de Janeiro. He was with the Industrial Engineering Dept. of Polo Universitário de Rio das Ostras (PURO) - UFF, in 2012-2013, as an Assistant Professor, and with INESC Porto, Portugal, as a Ph.D. student, in 2013. Currently, he is with the E. E. Dept. - UFF, as an Adjunct Professor. His research interests include computer methods and intelligent systems applied to electrical power grids.

Thiago Trezza Borges holds a bachelor's degree (2004) and a master's degree (2006) in Electrical Engineering at the Federal University of Juiz de Fora (UFJF) and a Ph.D. (2012) at the Federal University of Rio de Janeiro (UFRJ/COPPE), Brazil. Since 2005, he has been working at PETROBRAS as an equipment engineer, and since 2013, he has been a professor at the Fluminense Federal University (UFF). He is interested in the following research areas: optimization of industrial electrical systems, distribution, and transmission.

André Fernando Schiochet was born in Brazil in 1979. He holds a Bachelor's degree (2003) and a Master's degree (2006) in Electrical Engineering, both from the Federal University of Santa Catarina (UFSC). In 2021, he began his Ph.D. in Electrical Engineering at the Federal University of Juiz de Fora (UFJF), Minas Gerais. Since 2008, he has been an equipment engineer at Petrobras and, since 2014, a professor at Petrobras University, Brazil. His research interests include renewable energy, energy storage systems, electrical studies, and the development of tools for the optimization of industrial systems, generation, transmission, and distribution.